Identification of Pacific Ocean sea surface temperature influences of Upper Colorado River Basin snowpack

Oubeidillah A. Aziz,[1] Glenn A. Tootle,[1] Stephen T. Gray,[2] and Thomas C. Piechota[3]

Received 31 March 2009; revised 23 December 2009; accepted 19 January 2010; published 27 July 2010.

[1] Given the importance of Upper Colorado River Basin (UCRB) snowpack as the primary driver of streamflow (water supply) for the southwestern United States, the identification of Pacific Ocean climatic drivers (e.g., sea surface temperature (SST) variability) may prove valuable in long-lead-time forecasting of snowpack in this critical region. Previous research efforts have identified El Niño–Southern Oscillation (ENSO) and Pacific Decadel Oscillation (PDO) as the main drivers for western U.S. snowpack, but these drivers have limited influence on regional (Utah and Colorado) UCRB snowpack. The current research applies for the first time the Singular Value Decomposition (SVD) statistical method to Pacific Ocean SSTs and continental U.S. snowpack to identify the primary Pacific Ocean climatic driver of UCRB snowpack. The use of SSTs eliminates any "bias" as to specific climate signals. The second mode of SVD identified a UCRB snowpack region (Colorado and Utah) and a corresponding Pacific Ocean SST region. A "non-ENSO/non-PDO" Pacific Ocean SST region between 34°N–24°S and 150°E–160°W was identified as being the primary driver of UCRB snowpack. To confirm the UCRB snowpack results, data from 13 unimpaired (or naturalized) streamflow gages in Colorado and Utah were used to evaluate and support the snowpack findings. Finally, a new and beneficial data set (western U.S. 1 March, 1 April, and 1 May snow water equivalent) was developed, which may be used in future research efforts.

Citation: Aziz, O. A., G. A. Tootle, S. T. Gray, and T. C. Piechota (2010), Identification of Pacific Ocean sea surface temperature influences of Upper Colorado River Basin snowpack, *Water Resour. Res.*, *46*, W07536, doi:10.1029/2009WR008053.

1. Introduction

[2] Numerous investigations have evaluated oceanic-atmospheric variability and continental U.S. hydrologic (e.g., streamflow, precipitation and snowpack) response [*Hunter et al.*, 2006; *Tootle et al.*, 2005; *Rogers and Coleman*, 2003; *McCabe and Dettinger*, 2002; *Enfield et al.*, 2001; *Cayan et al.*, 1999; *Gershunov*, 1998; *Kahya and Dracup*, 1993; *Cayan and Webb*, 1992; *Cayan and Peterson*, 1989] with the possible goal of using climatic variables as a predictor [*Soukup et al.*, 2009; *Grantz et al.*, 2005; *Tootle and Piechota*, 2004]. These studies show strong subcontinental impacts linked to particular phases (e.g., cold or warm) of Pacific Ocean climate variability (e.g., El Niño–Southern Oscillation (ENSO) and the Pacific Decadal Oscillation (PDO)). Therefore, the current research will concentrate on Pacific Ocean variability precisely because the mechanistic links to western North American snowpack are better understood than those with Atlantic and/or Indian Ocean variability. Additionally, in the western United States, the primary source of water for municipal, agricultural and hydropower use is snowpack. This is primarily attributed to precipitation occurring in the form of snowfall and, in the western United States, snowfall accounts for approximately 50 to 70% of total annual precipitation [*Clark et al.*, 2001].

[3] A previous study applied multivariate and correlation statistical techniques to western U.S. snowpack data, attempting to identify Pacific Ocean climatic variability in snowpack (snow water equivalent or SWE). *McCabe and Dettinger* [2002] applied Principal Components Analysis (PCA) to 1 April SWE for 323 western U.S. stations. The two primary modes (components) accounted for 61% of the total snowpack variability in the western United States. Interestingly, the first mode of snowpack variability closely represented the PDO while the second mode represented both PDO and ENSO. However, when utilizing correlation analysis, neither an ENSO or PDO signal was identified in Upper Colorado River Basin (UCRB) (Utah and Colorado) snowpack [*McCabe and Dettinger*, 2002]. Given that ENSO and PDO are not the primary Pacific Ocean climatic drivers of UCRB (Utah and Colorado) snowpack, the motivation of the current research is to identify what Pacific Ocean climatic variability is associated with UCRB (Utah and Colorado) snowpack variability. To investigate this, Pacific Ocean sea surface temperatures (SSTs) are selected and Singular Value Decomposition (SVD) is applied.

[4] SVD is a powerful technique that *Bretherton et al.* [1992] concluded was simple to use and preferable for general use, while *Wallace et al.* [1992] found SVD isolates the most important modes of variability. SVD has been

[1]Department of Civil and Environmental Engineering, University of Tennessee, Knoxville, Tennessee, USA.
[2]Wyoming Water Resources Climate Data System and Wyoming State Climate Office, University of Wyoming, Laramie, Wyoming, USA.
[3]Department of Civil and Environmental Engineering, University of Nevada, Las Vegas, Nevada, USA.

0043-1397/10/2009WR008053

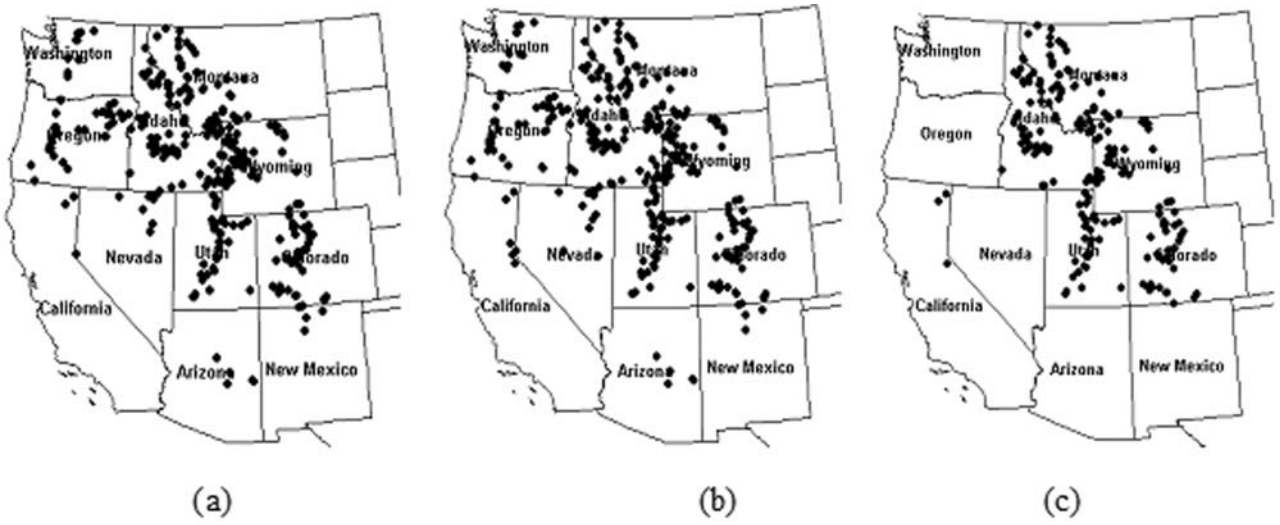

Figure 1. Location map of snow water equivalent (SWE) stations for (a) 1 March, (b) 1 April, and (c) 1 May.

utilized to evaluate SST and hydrologic variability [*Tootle et al.*, 2008; *Tootle and Piechota*, 2006; *Shabbar and Skinner*, 2004; *Rodriguez-Fonseca and de Castro*, 2002; *Rajagopalan et al.*, 2000; *Wang and Ting*, 2000; *Giannini et al.*, 2000; *Enfield and Alfaro*, 1999; *Uvo et al.*, 1998]. While several of these studies investigated SST and hydrologic variability (e.g., Palmer Drought Severity Index (PDSI), precipitation, streamflow) in the United States and Canada, this research is a comprehensive (e.g., three predictor periods and three predictand periods) and first-time investigation of Pacific Ocean SSTs and western U.S. snowpack. While PCA is very useful in data reduction when working with one spatial-temporal field, the SVD approach used in this analysis has the advantage of evaluating the cross-covariance matrix of two spatial-temporal fields to identify regions of similar behavior. Additionally, the use of SVD with SSTs and SWE does not limit the investigator to predefined (e.g., ENSO, PDO) regions of climate variability and the resulting SWE response to phases (e.g., warm or cold) of these climate signals. Therefore, the contributions of the current research are (1) the development of a new data set of western U.S. snowpack (SWE) for 1 March, 1 April, and 1 May; (2) a comprehensive (i.e., three predictor periods and three predictands) first-time analysis of Pacific Ocean SST and western U.S. snowpack variability; (3) the identification of the Pacific Ocean SST regions that influence western U.S. snowpack; and (4) the verification of these Pacific Ocean SST regions of influence in an alternate hydrologic variable (e.g., UCRB streamflow).

2. Data and Methodology

[5] Historic 1 March, 1 April, and 1 May SWE data were obtained from the Natural Resources Conservation Service (NRCS) website (http://www.wcc.nrcs.usda.gov/snotel/) for snow measurement stations in the western United States. A tradeoff between the period of record length (temporal dimension) and the number of snowpack stations (spatial dimension) resulted in 291 (1 March), 323 (1 April) and 216 (1 May) snowpack stations being identified with a period of record 1961 to 2006 (46 years) (Figure 1). Each of the snowpack stations used in the current research had complete records and the 1 April SWE data set has been used in previous research efforts [*Hunter et al.*, 2006]. Both the temporal (46 years) and spatial (number of stations) dimensions were consistent with previously published studies utilizing SVD with SSTs and hydrologic variables [*Tootle et al.*, 2008; *Tootle and Piechota*, 2006; *Uvo et al.*, 1998].

[6] Pacific Ocean SST data were obtained from the National Climatic Data Center website (http://www.cdc.noaa.gov/cdc/data.noaa.erSST.html) [*Smith and Reynolds*, 2002]. This data set consists of monthly average values at a resolution of 2° by 2° and ranges from latitude 20° south to 60° north and 120° east to 80° west. This resulted in 2,792 active Pacific Ocean SST cells. Average Pacific Ocean SSTs were calculated for three different 6 month windows (January–June or JFMAMJ, April–September or AMJJAS, and July–December or JASOND) preceding each snow season. This resulted in lead times varying from 2 months to 10 months. For both the Pacific Ocean SSTs and SWE data sets, anomalies, defined as the deviation of the seasonal mean from the long time average, were calculated and then standardized. These standardized anomalies of the data sets were used in this study. Thus, the detrending was based on the least squares fit of a straight line to the data sets and subtracting the resulting function from the data. Detrending the SST and snowpack data removes any trends in the data sets that may bias the analysis and mask the underlying variability.

[7] Two of the applicable predefined data sets representing oceanic-atmospheric climatic phenomena are the Niño 3.4 index (ENSO) and the PDO index. The average monthly values for the climatic indices (Niño 3.4 and PDO) were averaged for each of the 6 month (e.g., JFMAMJ, AMJJAS, JASOND) predictor periods. The Niño 3.4 [*Trenberth*, 1997] SST region is located along the equatorial Pacific Ocean (5°S–5°N, 170°–120°W). Monthly index Nino 3.4 data were obtained from the NOAA ESRL Physical Sciences Division (http://www.cdc.noaa.gov/Pressure/Timeseries/Nino34/). The Niño 3.4 index was used since it is an overall repre-

sentation of ENSO. The PDO is a oceanic/atmospheric phenomenon associated with persistent, bimodal climate patterns in the northern Pacific Ocean (poleward of 20° north) that oscillate with a characteristic period on the order of 50 years (a particular phase of the PDO will typically persist for about 25 years) [*Mantua et al.*, 1997; *Mantua and Hare*, 2002]. PDO Index [*Mantua et al.*, 1997; *Hare and Mantua*, 2000] values were obtained from the Joint Institute for the Study of the Atmosphere and Ocean, University of Washington (http://tao.atmos.washington.edu/pdo/).

[8] SVD is a powerful statistical tool for identifying coupled relationships between two, spatial-temporal fields. While *Bretherton et al.* [1992] provide a detailed discussion of the theory of SVD, a brief description of SVD as applied in this study, is provided. Initially, a matrix of standardized SST anomalies and a matrix of standardized SWE anomalies were developed. Please note that an individual SST anomaly matrix is developed for each predictor period (one matrix each for JFMAMJ, AMJJAS and JASOND Pacific Ocean SSTs) and an individual SWE anomaly matrix is developed for each predictand (one matrix each for 1 March, 1 April and 1 May SWE). This results in the development of three predictor (SST) matrices and three predictand (SWE) matrices. The time dimension of each matrix (i.e., 46 years) must be equal while the spatial component (i.e., the number of SST cells and the number of SWE stations) can vary in dimension. The cross-covariance matrix was then computed for the two spatiotemporal matrices and SVD was applied to the cross-covariance matrix and "teleconnection" information regarding the relationship between the two was obtained. A total of nine cross-covariance matrices resulted, representing all combinations of the three predictors (SSTs) and three predictands (SWE).

[9] The resulting SVD of each cross-covariance matrix created two matrices of singular vectors and one matrix of singular values. The singular values were ordered such that the first singular value (first mode) was greater than the second singular value and so on. *Bretherton et al.* [1992] defines the squared covariance fraction (SCF) as a useful measurement for comparing the relative importance of modes in the decomposition. Each singular value was squared and divided by the sum of all the squared singular values to produce a fraction (or percentage) of squared covariance for each mode. In applying SVD, the SCF is somewhat analogous to the percent of explained variance (by components) when applying PCA.

[10] Finally, the two matrices of singular vectors were examined, generally referred to as the left (i.e., SST) matrix and the right (i.e., SWE) matrix. The first column of the left matrix (first mode) was projected onto the standardized SST anomalies matrix and the first column of the right matrix (first mode) was projected onto the standardized SWE anomalies matrix. This resulted in the first temporal expansion series (TES) of the left and right fields, respectively. The left heterogeneous correlation field (for the first mode) was determined by correlating the SST values of the left matrix with first temporal expansion series of the right field and the right heterogeneous correlation field (for the first mode) was determined by correlating the SWE values of the right matrix with the first temporal expansion series of the left field. The left temporal expansion series have a physical meaning since they represent SST variability that may not already be included in existing SST indices and could represent a new index of SST variability. This procedure is then repeated for the second and third modes. While a 90% level of significance was used in previous research efforts [*Tootle et al.*, 2008], a threshold value of 95% significance was established for the current research, and maps displaying significant correlation values for SWE regions and Pacific Ocean SSTs regions are provided.

[11] While SVD is a powerful tool for the statistical analysis of two spatiotemporal fields, there exist several limitations to its use that should be investigated [*Newman and Sardeshmukh*, 1995]. However, if the leading (first, second, third) modes explain a significant amount of the variance of the two fields, then SVD can be applied to determine the strength of the coupled variability present [*Newman and Sardeshmukh*, 1995].

3. Results

[12] The use of three Pacific Ocean SST predictor periods (JFMAMJ, AMJJAS and JASOND) and three SWE predictands (1 March, 1 April and 1 May) resulted in square covariance fractions ranging from 42% to 78% for the first mode; 8% to 31% for the second mode; and 4% to 14% for the third mode (Figure 2). In the resulting nine individual analyses, the leading (first, second and third) modes explained, together, a minimum of 82% to a maximum of 92% of the variance. Thus, SVD can be used in the analysis [after *Newman and Sardeshmukh*, 1995]. For Figures 3–5, blue represents negative correlation values, while red represents positive correlation values above the 95% significance level. Nonsignificant snowpack stations are represented by black dots. Only 1 April snowpack (and Pacific Ocean SSTs) results are presented below in the current research as similar spatial patterns (and significance levels) were observed in 1 March and 1 May snowpack (and Pacific Ocean SSTs). Finally, an additional analysis was performed such that the Pacific Ocean SST data were weighted by the square root of cosine of latitude to account for spatial variations of the grid cells. Similar to the work of *Wallace et al.* [1992], the results did not show any noticeable differences.

3.1. SVD First Mode: Pacific Ocean SSTs (JFMAMJ, AMJJAS, JASOND) and Western U.S. 1 April SWE

[13] First, a distinct Pacific Ocean equatorial SST pattern (e.g., ENSO) was observed and this pattern appears to intensify as the lead time between the SST period and the SWE date reduces (Figure 3). This ENSO-like pattern was verified through the use of correlation analysis. The SVD SST first TES for all three predictor seasons (JFMAMJ, AMJJAS and JASOND) and 1 April snowpack were correlated with the seasonal average Niño 3.4 index for the corresponding (matching) SST season. The magnitude of the correlation values ranged from 0.81 to 0.93, which is evident in the plot of the first TES and the Niño 3.4 (and PDO) indices (Figure 3). Thus, the ENSO signal was present and identified (verified) in the observed Pacific Ocean SST spatial patterns. A similar correlation analysis was performed with the seasonal average of PDO for the corresponding (matching) predictor season. The magnitude of the correlation values ranged from 0.54 to 0.65. On the basis of the correlation analysis, the ENSO signal appears to have a stronger relationship (higher correlation values) than the

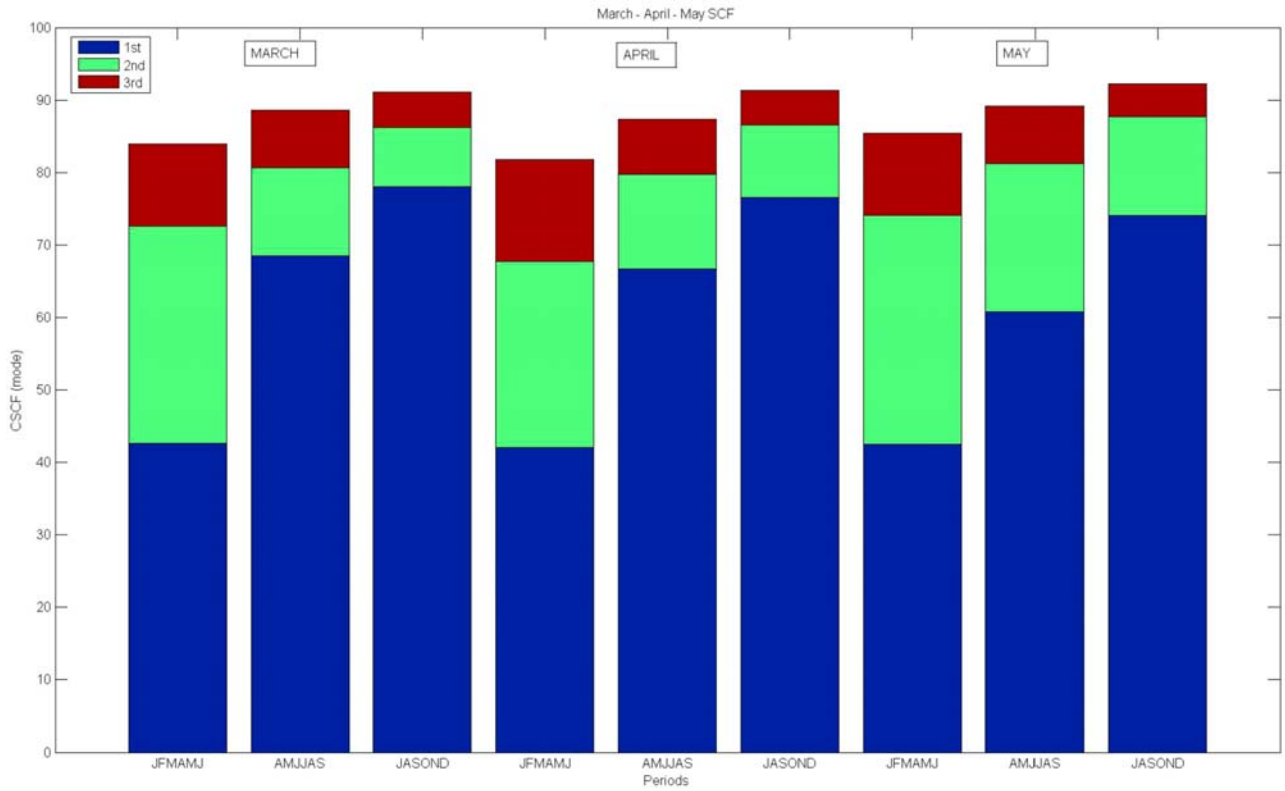

Figure 2. Cumulative Squared Covariance Fractions (CSCF) for 1 March, 1 April, and 1 May SWE (1961–2006) and Pacific Ocean SST (1960–2005) predictor periods (JFMAMJ, AMJJAS, and JASOND). Blue, green, and red represent first mode, second mode, and third mode, respectively.

PDO signal in western U.S. snowpack, for the stations identified as being significant in the first mode.

[14] Also, more important is the relationship the SST pattern exhibits with western U.S. snowpack. As previously discussed, while negative and positive regions are displayed for both Pacific Ocean SSTs and SWE stations, it is important to understand that the signs (+/−) of the correlation values represent how the Pacific Ocean SST regions interact with the western U.S. SWE stations. Pacific Ocean SST regions and SWE stations that exhibit the same color (sign) have a positive relationship and behave similarly. As such increased (decreased) Pacific Oceans SSTs result in increased (decreased) SWE. However, if the signs are opposite for the Pacific Ocean SST regions and SWE stations, they will behave in an opposite manner (i.e., increased (decreased) Pacific Oceans SSTs result in decreased (increased) SWE).

[15] Interestingly, a distinct ENSO-like SWE response was identified in western U.S. snowpack such that a warming (cooling) of equatorial SSTs results in a decrease (increase) in Pacific Northwest snowpack. While SWE stations are limited in the southwestern United States, a similar ENSO-like pattern was observed such that a warming (cooling) of equatorial SSTs results in an increase (decrease) in Southwest snowpack.

[16] However, most notable is that a consistent pattern of nonsignificant UCRB (Utah and Colorado) snowpack stations were identified. Therefore, it appears that ENSO (and PDO) are not the primary Pacific Ocean climatic drivers of snowpack in this region. In an attempt to identify the Pacific Ocean climatic drivers of snowpack in this region, the results of the SVD second mode were examined.

3.2. SVD Second Mode: Pacific Ocean SSTs (JFMAMJ, AMJJAS, JASOND) and Western U.S. 1 April SWE

[17] First, a distinct SST pattern was observed in the western Pacific Ocean (east of Japan) and no "ENSO-like" or "PDO-like" SST patterns were identified. Next, the "missing" SWE region (i.e., UCRB; Utah and Colorado) of SWE stations (from the SVD first mode) was identified as significant in the SVD second mode (Figure 4). It appears that an increase (decrease) in SST in this Pacific Ocean region east of Japan results in a decrease (increase) in UCRB SWE. While ENSO (and to some degree, PDO) are recognized as the primary climatic drivers of western U.S. snowpack, the UCRB region (UT and CO) appears to be driven by this SST region. This is also evident in the plot of the second TES and the Niño 3.4 (and PDO) indices, in which lower correlations (when compared to the first TES) are observed (Figure 4). Please note, the "switching" of the signs is inherent to SVD, and the importance of the results is the positive/negative relationships between SSTs regions and SWE stations, as displayed by Figure 4.

[18] To further investigate the Pacific Ocean SST region identified in the second mode, the SVD analysis was performed on a subset of 1 April snowpack stations. Fifty-four (54) 1 April snowpack stations were selected in Colorado and Utah and SVD was performed using the same three predictor periods for Pacific Ocean SSTs. Interestingly, the

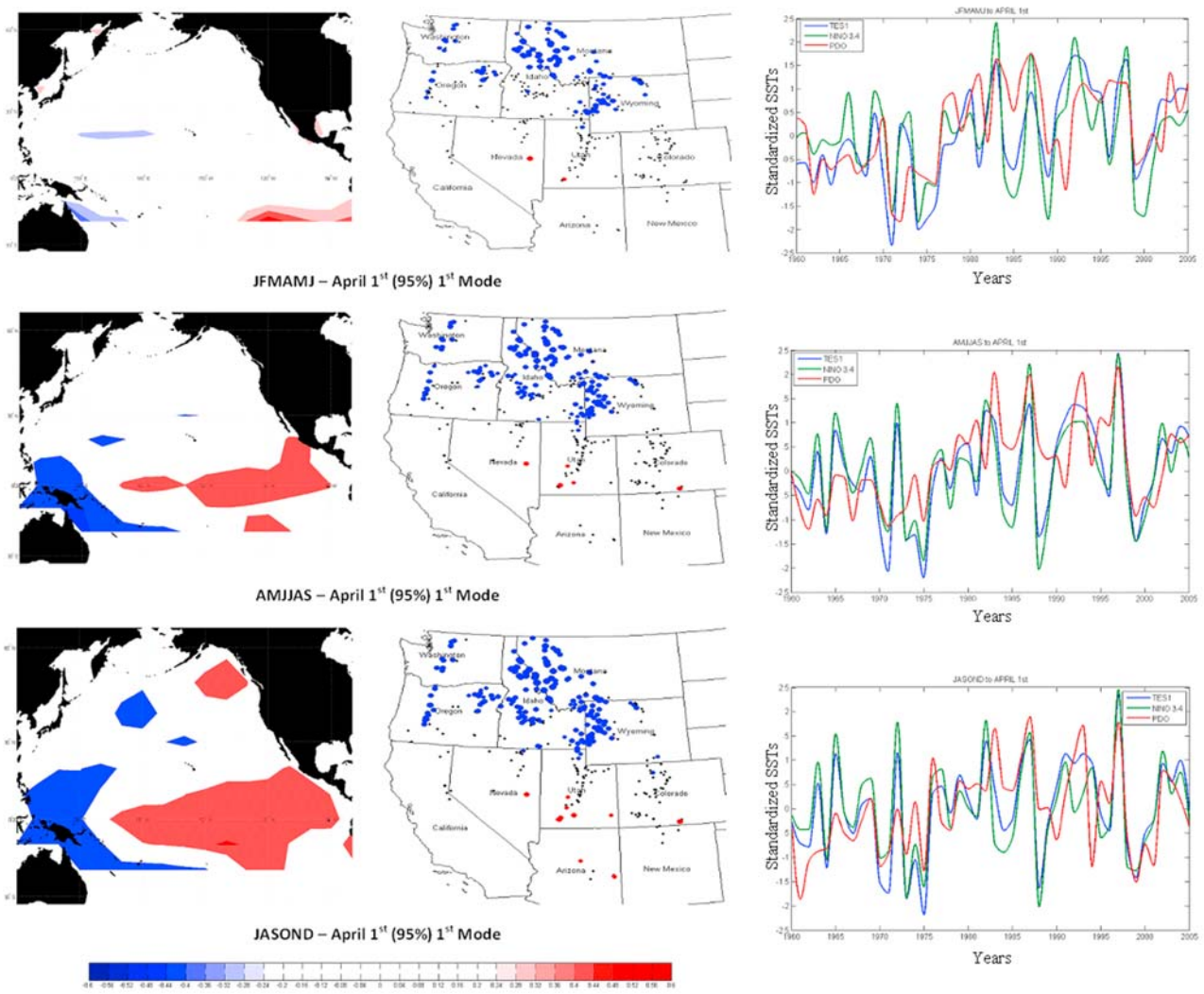

Figure 3. Heterogeneous correlation images (first mode) when applying Singular Value Decomposition (SVD) to the previous year's (1960–2005) Pacific Ocean SSTs for (a) JFMAMJ, (b) AMJJAS, and (c) JASOND, and current year (1961–2006) 1 April SWE. Negative (positive) correlations (95% significance) are represented by blue (red). Nonsignificant snowpack stations are represented by black dots. Time series plot of seasonal first Temporal Expansion Series (TES1), Niño 3.4 index, and PDO index is also shown.

results of this analysis (first mode) displayed similar spatial SST and snowpack regions as the previous results (Figure 4). Next, an additional analysis of 13 reconstructed streamflow (water year) gages in the UCRB (Utah and Colorado) with a period of record of 1861 to 1990 and Pacific Ocean SSTs with period of record of 1860 to 1989 was conducted. The results supported the findings from the snowpack analysis in Figure 4 (second mode) and the previous 54 station snowpack analysis in that a similar Pacific Ocean SST region was identified and all 13 streamflow gages were determined to be significant. Finally, previous research efforts [*Uvo et al.*, 1998; *Wang and Ting*, 2000; *Shabbar and Skinner*, 2004; *Tootle and Piechota*, 2006; *Tootle et al.*, 2008] had large spatial differences between SSTs (i.e., number of cells) and hydrologic variables (i.e., number of gages). To assure the current results were not due to the Pacific Ocean SST field overwhelming the snowpack field, an additional analysis was performed such that the Pacific Ocean SST region (34°N to 24°S and 150°E to 160°W) identified in the second mode (Figure 4) was isolated such that only that region was used in SVD with western U.S. snowpack. The intent is to reduce the SST spatial component (i.e., number of cells) such that it is similar in size to the snowpack spatial component (i.e., number of snowpack stations). The results supported the current research efforts in that UCRB (Utah and Colorado snowpack region) was identified in the first mode. This represents an important discovery as confirmed in the following validation analysis.

3.3. Validation Analysis

[19] To confirm the results for the current research, which evaluated three, 6 month predictor periods, an additional analysis was performed using four, 3 month predictor periods for the Pacific Ocean SSTs (December–January–February (DJF), March–April–May (MAM), June–July–

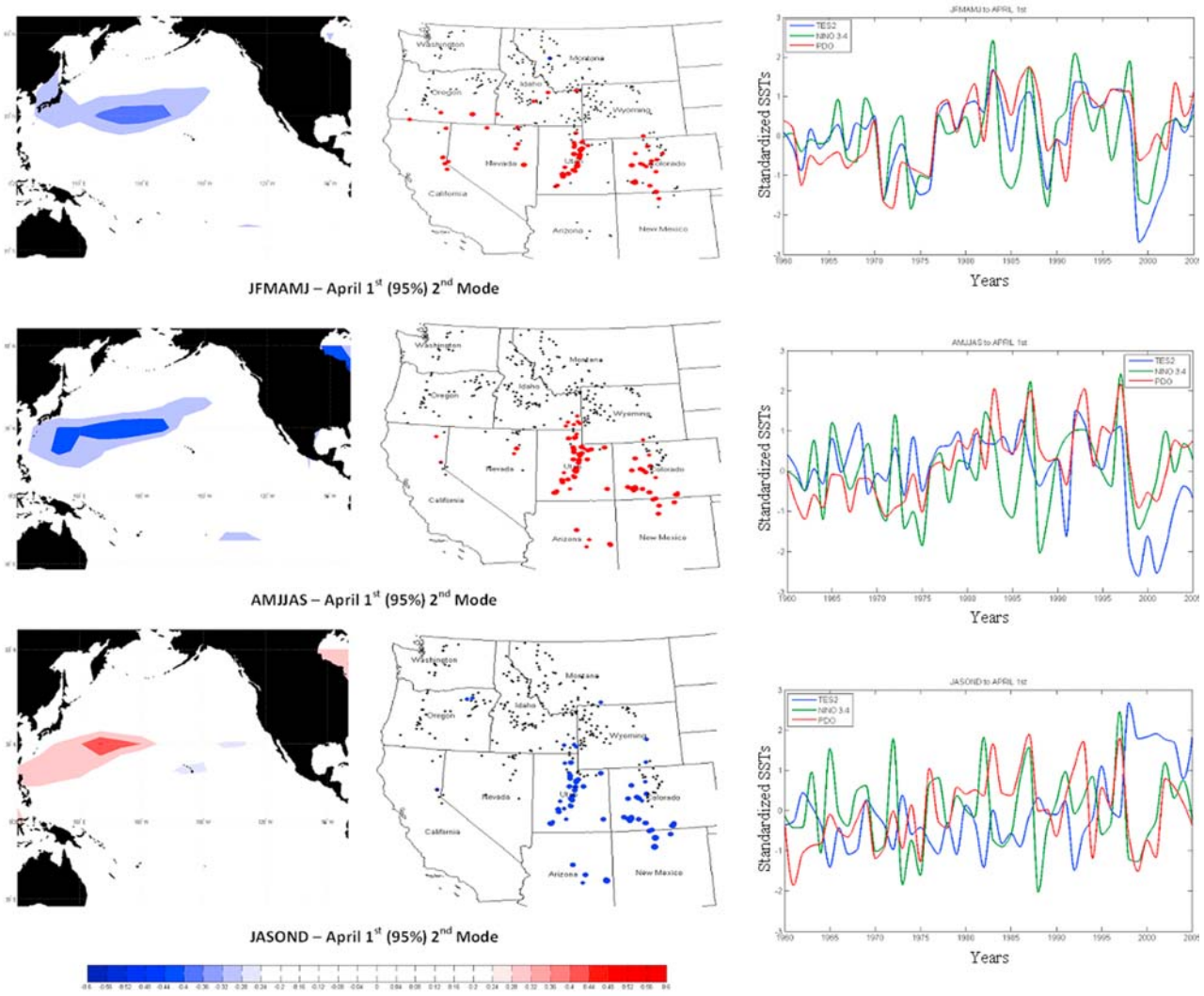

Figure 4. Heterogeneous correlation images (second mode) when applying SVD to the previous year's (1960–2005) Pacific Ocean SSTs for (a) JFMAMJ, (b) AMJJAS, and (c) JASOND, and current year (1961–2006) 1 April SWE. Negative (positive) correlations (95% significance) are represented by blue (red). Nonsignificant snowpack stations are represented by black dots. Time series plot of seasonal second Temporal Expansion Series (TES2), Niño 3.4 index, and PDO index is also shown.

August (JJA) and September–October–November (SON)). The results of the first mode and the second mode revealed similar spatial patterns for both Pacific Ocean SSTs and snowpack as displayed in the current research.

[20] The Pacific Ocean SST region identified by the SVD second mode extends from approximately 34°N to 24°S and 150°E to 160°W (Figure 4). A yearly (1960 to 2005), seasonal (JFMAMJ, AMJJAS, JASOND) SST index for this region, analogous to the Niño 3.4 index representing ENSO strength, were created by seasonally averaging all the cells within that region per year. Following the procedure outlined by *McCabe and Dettinger* [2002], the three seasonal (JFMAMJ, AMJJAS, JASOND) SST averages for the 34°N to 24°S and 150°E to 160°W spatial region were correlated with 1 April SWE. This results in three maps (Figure 5) that display correlations exceeding the 95% confidence level. The results are very similar to Figure 4 in that the UCRB SWE stations are identified as being significant while northwestern and southwestern U.S. SWE stations are not significant. Additionally, the SWE stations identified as being significant are negatively correlated with the SST region, thus verifying the results from the SVD analysis that an increase (decrease) in SST temperatures in this region results in a decrease (increase) in UCRB SWE. The resulting correlation analysis (Figure 5) displays significant SWE stations that were not identified as significant by *McCabe and Dettinger* [2002], who used (only) ENSO and PDO indices.

[21] As performed by *Watson et al.* [2009], spectral analysis [*Torrence and Compo*, 1998] reveals that the first TES displays a higher-frequency signal (approximately 4 to 6 years) while the second TES does not display a similar higher-frequency signal (Figure 6). The higher-frequency signal in the first TES is most likely associated with ENSO. A visual comparison of the spectral analysis of the first TES

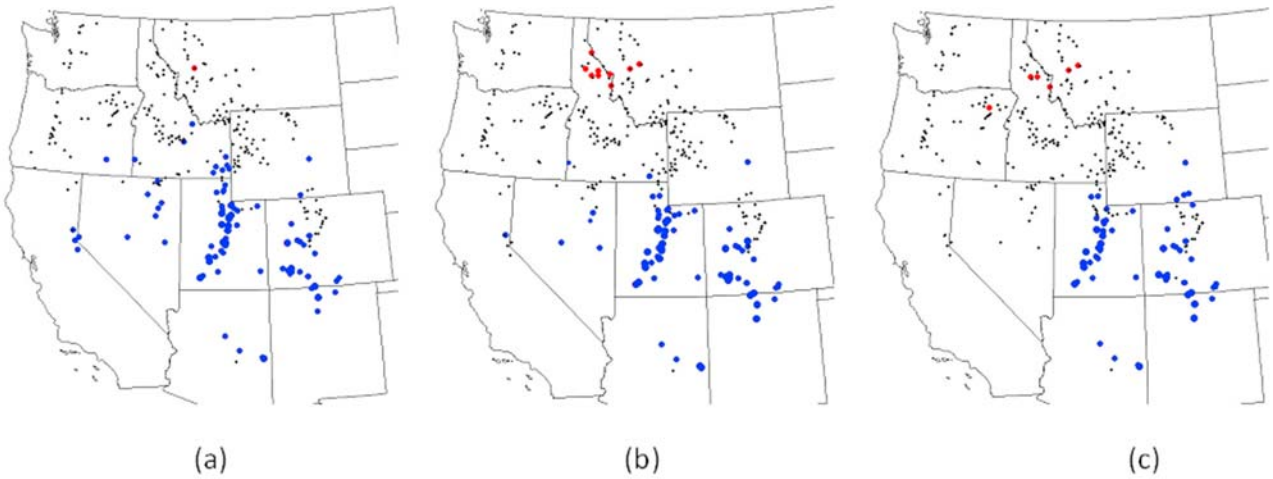

Figure 5. Correlation maps for yearly (1960–2005), seasonal (a) JFMAMJ, (b) AMJJAS, and (c) JASOND, Pacific Ocean SST region (34°N–24°S and 150°E–160°W) and yearly (1961–2006) 1 April SWE. Negative (positive) correlations (95% confidence level) are represented by blue (red) dots, while nonsignificant correlations are represented by black dots.

and the Niño 3.4 index for the same season (AMJJAS) and period of record displayed similar patterns.

4. Discussion and Conclusions

[22] A thorough (three predictor periods, three predictands, two modes) investigation of Pacific Ocean SSTs and western U.S. snowpack resulted in the development of a comprehensive SWE data set and the "possible first-time" identification of the primary Pacific Ocean driver of UCRB snowpack. However, has this Pacific Ocean SST pattern been previously observed and perhaps overlooked owing to the focus on ENSO and PDO? *Rajagopalan et al.* [2000] utilized SVD to evaluate global SSTs and continental U.S. PDSI for several periods including 1963 to 1995 (similar period of record to the current research). While the authors of the current research acknowledge there is considerable more "noise" in the *Rajagopalan et al.* [2000] analysis (global SSTs instead of Pacific Ocean SSTs and continental U.S. PDSI instead of western U.S. SWE), *Rajagopalan et al.* [2000] identified a similar spatial Pacific Ocean SST pattern (east of Japan). Also, this SST pattern was equal in strength (correlation significance) to the ENSO-like pattern that was concurrently identified. Thus, it appears that a significant non-ENSO climatic driver, similar to the current research, was identified by *Rajagopalan et al.* [2000]. *Wang and Ting* [2000] utilized SVD to evaluate Pacific Ocean SSTs and continental U.S. precipitation from 1951 to 1994. Again, while the authors of the current research recognized the increased "noise" (continental U.S. precipitation instead of western continental U.S. snowpack) of this data set, a similar Pacific Ocean SST pattern (east of Japan) was simultaneously identified with an ENSO-like pattern. Similar to *Rajagopalan et al.* [2000], this SST pattern was equal in strength to the ENSO like pattern. *Grantz et al.* [2005] identified a similar Pacific Ocean SST pattern and no ENSO-like SST pattern when developing predictors for long-lead-time forecasts of the Truckee-Carson River system, located in eastern California and western Nevada, near Lake Tahoe. The physical explanation for this Pacific Ocean SST region that was provided by *Grantz et al.* [2005] was based on a composite analysis of average SST, wind and 500 mbar pressure patterns, focusing on high- and low- (extreme) streamflow years. *Grantz et al.* [2005] concluded

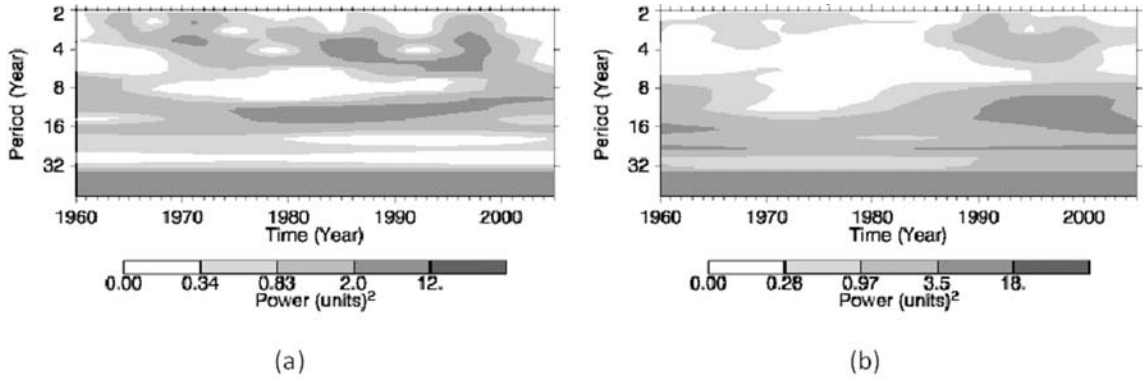

Figure 6. Wavelet power spectra for the SVD (a) first Temporal Expansion Series and (b) second Temporal Expansion Series for previous year AMJJAS Pacific Ocean SSTs (1960–2005) and current year 1 April SWE (1961–2006).

that the SST patterns in high- and low-streamflow years were a direct response to pressure and winds, resulting in evaporative cooling that results in cooler than normal SSTs in this region. *Tootle and Piechota* [2006] utilized SVD to evaluate Pacific Ocean SSTs and continental U.S. streamflow for 1951 to 2002. Again, given the increase in data set "noise" (continental U.S. streamflow instead of western continental U.S. snowpack), a similar Pacific Ocean SST pattern (east of Japan) was simultaneously identified with a ENSO-like pattern and, the SST pattern displayed higher strength (correlation significance) than the ENSO-like pattern. Finally, *Soukup et al.* [2009] extended the work of *Grantz et al.* [2005], utilizing SVD (in lieu of correlation techniques) to identify long-lead-time predictors (SSTs) of North Platte River streamflow and identified a similar Pacific Ocean SST pattern. While *Grantz et al.* [2005] and *Soukup et al.* [2009] appeared to capture (isolate) this Pacific Ocean SST pattern without a concurrent ENSO-like pattern, the current research represents the first time this pattern has been associated with UCRB (Utah and Colorado) hydrology (both snowpack and streamflow). The ability to isolate this pattern in the work of *Grantz et al.* [2005] and *Soukup et al.* [2009] and the current research efforts can most likely be attributed to the loss of "noise" (i.e., smaller spatial regions – Truckee-Carson River System and North Platter River Basin) in the predictand data set. Additionally, these predictand regions tend to be aligned along the 40° North parallel and may reflect the "switching or turning axis" of acknowledged hydrologic response to ENSO.

[23] In particular, the use of SVD on SST fields covering the majority of the Tropical and North Pacific Ocean rather than a predefined SST subregion (e.g., Nino 3.4) eliminates important biases associated with the use of composite climatic indices. An analysis of spatial patterns in the mapped correlation fields (Figure 3) provided an independent confirmation of ENSO and PDO-like patterns. However, while *McCabe and Dettinger* [2002] identified the PDO as the slightly more dominant signal, the current research found ENSO to be slightly more dominant on the basis of correlation analysis. This is most likely due to SVD requiring the use of a defined (seasonal 6 month SST) predictor period. Although the current research evaluates a 46 year period of record, 6 month predictor periods would most likely capture an interannual (high frequency) climate signal (e.g., ENSO) versus and interdecadal (low frequency) climate signal (e.g., PDO). While the current research was limited to evaluating Pacific Ocean SSTs, other climatic variables (e.g., 500 mbar anomalies) may provide additional insight into the physical mechanisms and drivers of UCRB snowpack.

[24] *McCabe and Dettinger* [2002], through the use of correlation analysis, showed ENSO and PDO were not identified in UCRB (Utah and Colorado) snowpack. However, owing to the limitation of using climate indices (only), no explanation could be provided as to what Pacific Ocean SST regions drive UCRB snowpack. The current research accomplished this when evaluating the SVD second mode (Figures 4 and 5). While only 1 April SWE results are provided, for all three predictor and three predictant periods, a consistent Pacific Ocean SST pattern east of Japan was identified. This was further verified in streamflow data from Utah and Colorado. A similar pattern was verified in other research efforts [e.g., *Rajagopalan et al.*, 2000; *Wang and Ting*, 2000; *Grantz et al.*, 2005; *Tootle and Piechota*, 2006; *Soukup et al.*, 2009], but the importance of this Pacific Ocean SST region as a possible driver of UCRB hydrology (both SWE and streamflow) was not advocated in these research efforts.

[25] **Acknowledgments.** This research is supported by the USGS 104B program, the Wyoming Water Research Program, the Wyoming Water Development Commission, and the Ivanhoe Foundation Fellowship. Additional support is provided by the University of Tennessee, Knoxville Science Alliance/Oak Ridge National Laboratory Joint Directed Research and Development program. S. Gray was supported by the NSF Geography and Regional Science Program (grant 0620793). The research at UNLV is supported by grants NSF EPS-0814372, NOAA NA070AR4310228, DOE DE-FG02-08ER64709, and DOE DE-EE-0000716. The authors wish to thank the three anonymous reviewers for the helpful comments.

References

Bretherton, C. S., C. Smith, and J. M. Wallace (1992), An intercomparison of methods for finding coupled patterns in climate data, *J. Clim.*, *5*, 541–560, doi:10.1175/1520-0442(1992)005<0541:AIOMFF>2.0.CO;2.

Cayan, D. R., and D. H. Peterson (1989), The influence of North Pacific atmospheric circulation on streamflow in the west, in *Aspects of Climate Variability in the Pacific and the Western Americas*, *Geophys. Monogr. Ser.*, vol. 55, edited by D. H. Peterson, pp. 375–397, AGU, Washington, D.C.

Cayan, D. R., and R. H. Webb (1992), El Niño/Southern Oscillation and streamflow in the western United States, in *El Niño: Historical and Paleoclimatic Aspects of the Southern Oscillation*, pp. 29–68, Cambridge Univ. Press, New York.

Cayan, D. R., K. T. Redmond, and L. G. Riddle (1999), ENSO and hydrologic extremes in the Western U.S., *J. Clim.*, *12*, 2881–2893, doi:10.1175/1520-0442(1999)012<2881:EAHEIT>2.0.CO;2.

Clark, M. P., M. C. Serreze, and G. J. McCabe (2001), Historical effects of El Niño and La Niña events on seasonal evolution of the montane snowpack in the Columbia and Colorado River Basins, *Water Resour. Res.*, *37*(3), 741–757, doi:10.1029/2000WR900305.

Enfield, D. B., and E. J. Alfaro (1999), The dependence of Caribbean rainfall on the interaction of the Tropical Atlantic and Pacific Oceans, *J. Clim.*, *12*, 2093–2103, doi:10.1175/1520-0442(1999)012<2093:TDOCRO>2.0.CO;2.

Enfield, D. B., A. M. Mestas-Nuñez, and P. J. Trimble (2001), The Atlantic multidecadal oscillation and its relation to rainfall and river flows in the continental U.S., *Geophys. Res. Lett.*, *28*(10), 2077–2080, doi:10.1029/2000GL012745.

Gershunov, A. (1998), ENSO influence on influence on intraseasonal extreme rainfall and temperature frequencies in the contiguous United States: Implications for long-range predictability, *J. Clim.*, *11*, 3192–3203, doi:10.1175/1520-0442(1998)011<3192:EIOIER>2.0.CO;2.

Giannini, A., Y. Kushnir, and M. A. Cane (2000), Interannual variability of Caribbean rainfall, ENSO, and the Atlantic Ocean, *J. Clim.*, *13*, 297–311, doi:10.1175/1520-0442(2000)013<0297:IVOCRE>2.0.CO;2.

Grantz, K., B. Rajagopalan, M. Clark, and E. Zagona (2005), A technique for incorporating large-scale climate information in basin-scale ensemble streamflow forecasts, *Water Resour. Res.*, *41*, W10410, doi:10.1029/2004WR003467.

Hare, S., and N. Mantua (2000), Empirical evidence for North Pacific regime shifts in 1977 and 1989, *Prog. Oceanogr.*, *47*, 103–145.

Hunter, T., G. A. Tootle, and T. C. Piechota (2006), Oceanic-atmospheric variability and western U.S. snowfall, *Geophys. Res. Lett.*, *33*, L13706, doi:10.1029/2006GL026600.

Kahya, E., and J. A. Dracup (1993), U.S. streamflow patterns in relation to the El Niño/Southern Oscillation, *Water Resour. Res.*, *29*(8), 2491–2503, doi:10.1029/93WR00744.

Mantua, N. J., and S. R. Hare (2002), The Pacific Decadal Oscillation, *J. Oceanogr.*, *58*(1), 35–44, doi:10.1023/A:1015820616384.

Mantua, N. J., S. R. Hare, Y. Zhang, J. M. Wallace, and R. C. Francis (1997), A Pacific interdecadal climate oscillation with impacts on salmon production, *Bull. Am. Meteorol. Soc.*, *78*, 1069–1079, doi:10.1175/1520-0477(1997)078<1069:APICOW>2.0.CO;2.

McCabe, G. J., and M. D. Dettinger (2002), Primary modes and predictability of year-to-year snowpack variations in the western United States

from teleconnections with Pacific Ocean climate, *J. Hydrometeorol.*, *3*, 13–25, doi:10.1175/1525-7541(2002)003<0013:PMAPOY>2.0.CO;2.

Newman, M., and P. D. Sardeshmukh (1995), A caveat concerning singular value decomposition, *J. Clim.*, *8*, 352–360, doi:10.1175/1520-0442(1995)008<0352:ACCSVD>2.0.CO;2.

Rajagopalan, B., E. Cook, U. Lall, and B. K. Ray (2000), Spatiotemporal variability of ENSO and SST teleconnections to summer drought over the United States during the twentieth century, *J. Clim.*, *13*, 4244–4255, doi:10.1175/1520-0442(2000)013<4244:SVOEAS>2.0.CO;2.

Rodriguez-Fonseca, B., and M. de Castro (2002), On the connection between winter anomalous precipitation in the Iberian Peninsula and North West Africa and the summer subtropical Atlantic sea surface temperature, *Geophys. Res. Lett.*, *29*(18), 1863, doi:10.1029/2001GL014421.

Rogers, J. C., and J. S. M. Coleman (2003), Interactions between the Atlantic Multidecadal Oscillation, El Niño/La Niña, and the PNA in winter Mississippi Valley stream flow, *Geophys. Res. Lett.*, *30*(10), 1518, doi:10.1029/2003GL017216.

Shabbar, A., and W. Skinner (2004), Summer drought patterns in Canada and the relationship to global sea surface temperatures, *J. Clim.*, *17*, 2866–2880, doi:10.1175/1520-0442(2004)017<2866:SDPICA>2.0.CO;2.

Smith, T. M., and R. W. Reynolds (2002), Extended reconstruction of global sea surface temperatures based on COADS data (1854–1997), *J. Clim.*, *16*, 1495–1510.

Soukup, T., O. Aziz, G. Tootle, S. Wulff, and T. Piechota (2009), Incorporating climate into a long lead-time non-parametric streamflow forecast, *J. Hydrol.*, *368*, 131–142, doi:10.1016/j.jhydrol.2008.11.047.

Tootle, G. A., and T. C. Piechota (2004), Suwannee River long-range streamflow forecasts based on seasonal climate predictors, *J. Am. Water Resour. Assoc.*, *40*(2), 523–532, doi:10.1111/j.1752-1688.2004.tb01047.x.

Tootle, G. A., and T. C. Piechota (2006), Relationships between Pacific and Atlantic ocean sea surface temperatures and U.S. streamflow variability, *Water Resour. Res.*, *42*, W07411, doi:10.1029/2005WR004184.

Tootle, G. A., T. C. Piechota, and A. K. Singh (2005), Coupled oceanic/atmospheric variability and United States streamflow, *Water Resour. Res.*, *41*, W12408, doi:10.1029/2005WR004381.

Tootle, G. A., T. C. Piechota, and F. Gutierrez (2008), The relationships between Pacific and Atlantic Ocean sea surface temperatures and Colombian streamflow variability, *J. Hydrol.*, *349*, 268–276, doi:10.1016/j.jhydrol.2007.10.058.

Torrence, C., and G. P. Compo (1998), A practical guide to wavelet analysis, *Bull. Am. Meteorol. Soc.*, *79*, 61–78, doi:10.1175/1520-0477(1998)079<0061:APGTWA>2.0.CO;2.

Trenberth, K. E. (1997), The definition of El Niño, *Bull. Am. Meteorol. Soc.*, *78*, 2771–2777, doi:10.1175/1520-0477(1997)078<2771:TDOENO>2.0.CO;2.

Uvo, C. B., C. A. Repelli, S. E. Zebiak, and Y. Kushnir (1998), The relationships between tropical Pacific and Atlantic SST and northeast Brazil monthly precipitation, *J. Clim.*, *11*, 551–562, doi:10.1175/1520-0442(1998)011<0551:TRBTPA>2.0.CO;2.

Wallace, J. M., D. S. Gutzler, and C. S. Bretheron (1992), Singular value decomposition of wintertime sea surface temperature and 500-mb height anomalies, *J. Clim.*, *5*, 561–576, doi:10.1175/1520-0442(1992)005<0561:SVDOWS>2.0.CO;2.

Wang, H., and M. Ting (2000), Covariabilities of winter U.S. precipitation and Pacific sea surface temperatures, *J. Clim.*, *13*, 3711–3719, doi:10.1175/1520-0442(2000)013<3711:COWUSP>2.0.CO;2.

Watson, T., F. A. Barnett, S. Gray, and G. Tootle (2009), Reconstructed streamflow for the headwaters of the Wind River, Wyoming USA, *J. Am. Water Resour. Assoc.*, *45*(1), 224–236, doi:10.1111/j.1752-1688.2008.00274.x.

O. A. Aziz and G. A. Tootle, Department of Civil and Environmental Engineering, University of Tennessee, 73F Perkins Hall, Knoxville, TN 37996, USA. (oaziz@utk.edu; gtootle@utk.edu)

S. T. Gray, Wyoming Water Resources Data System, University of Wyoming, Dept. 3943, 1000 E University Ave., Laramie, WY 82071, USA. (sgray8@uwyo.edu)

T. C. Piechota, Sustainability and Multidisciplinary Research, Civil and Environmental Engineering, University of Nevada, 4505 Maryland Parkway, Box 451087, Las Vegas, NV 89154-1087, USA. (thomas.piechota@unlv.edu)